JFM RAPIDS
journals.cambridge.org/rapids

Intermittency route to self-excited chaotic thermoacoustic oscillations

Yu Guan[1], Vikrant Gupta[2] and Larry K. B. Li[1],†

[1]Department of Mechanical and Aerospace Engineering, The Hong Kong University of Science and Technology, Clear Water Bay, Hong Kong

[2]Guangdong Provincial Key Laboratory of Turbulence Research and Applications, Department of Mechanics and Aerospace Engineering, Southern University of Science and Technology, Shenzhen, PR China

In nonlinear dynamics, there are three classic routes to chaos, namely the period-doubling route, the Ruelle–Takens–Newhouse route and the intermittency route. The first two routes have previously been observed in self-excited thermoacoustic systems, but the third has not. In this experimental study, we present evidence of the intermittency route to chaos in the self-excited regime of a prototypical thermoacoustic system – a laminar flame-driven Rijke tube. We identify the intermittency to be of type II from the Pomeau–Manneville scenario through an analysis of (i) the probability distribution of the quiescent epochs between successive bursts of chaos, (ii) the first return map, and (iii) the recurrence plot. By establishing the last of the three classic routes to chaos, this study strengthens the universality of how strange attractors arise in self-excited thermoacoustic systems, paving the way for the application of generic suppression strategies based on chaos control.

Key words: chaos, bifurcation

1. Introduction

Despite extensive research, thermoacoustic instability remains a serious problem in many combustion devices, such as gas turbines and rocket engines. It arises from positive feedback between the heat-release-rate (HRR) oscillations of an unsteady flame and the pressure oscillations associated with the combustor acoustics (Poinsot 2017). If the HRR and pressure oscillations are sufficiently in phase, the flame can transfer energy to the acoustic modes via the Rayleigh mechanism, producing self-excited flow oscillations at the characteristic acoustic frequencies of the system (Juniper & Sujith 2018). Here the term 'self-excited' refers to oscillations that have saturated nonlinearly after the onset of thermoacoustic instability. Such thermoacoustic

† Email address for correspondence: larryli@ust.hk

oscillations are usually high in amplitude and can therefore exacerbate thermal and fatigue stresses, prompting costly shutdowns in land-based power generation systems and jeopardizing flight safety in aerospace propulsion systems (Lieuwen & Yang 2005). There is thus a need to better understand how self-excited thermoacoustic oscillations arise in combustion systems, so that they can be avoided or suppressed.

1.1. *Chaos in self-excited thermoacoustic systems*

In early studies, it was often assumed that self-excited thermoacoustic systems could oscillate only in period-1 limit cycles, with motion restricted to a single temporal frequency and a time-independent amplitude. Recent studies, however, have overturned this assumption, revealing the prevalence of complex nonlinear dynamics such as quasi-periodicity and chaos (Juniper & Sujith 2018; Huhn & Magri 2020).

The first evidence of chaos in a self-excited thermoacoustic system was reported by Keanini, Yu & Daily (1989), who used phase-space reconstruction to identify a strange attractor in the pressure oscillations of a ramjet combustor. The next two decades, however, saw only isolated reports of chaos in thermoacoustics (Sterling 1993; Fichera, Losenno & Pagano 2001; Lei & Turan 2009). It was not until the most recent decade that widespread evidence of chaos began to emerge, facilitated by the advent of more sophisticated analysis tools based on dynamical systems theory and complex networks (Juniper & Sujith 2018). To date, experimental and numerical evidence of chaos has been found in various self-excited thermoacoustic systems, ranging from turbulent combustors (Gotoda *et al.* 2011; Kabiraj *et al.* 2015; Guan *et al.* 2019*c*) to laminar combustors powered by assorted HRR sources, such as a single V flame (Vishnu, Sujith & Aghalayam 2015), a single slot flame (Kashinath, Waugh & Juniper 2014) and multiple conical flames (Boudy *et al.* 2012; Kabiraj *et al.* 2012), to name just a few.

It is important to note that chaos can arise not just after the onset of thermoacoustic instability, but also before it. In turbulent premixed combustors, for example, Nair *et al.* (2013) and Nair, Thampi & Sujith (2014) showed through determinism tests that the low-amplitude aperiodic fluctuations observed before the onset of high-amplitude (self-excited) periodic oscillations can contain signs of high-dimensional chaos, overturning the long-held assumption that such a state of combustion noise is purely stochastic (Tony *et al.* 2015). Transition to thermoacoustic instability in turbulent combustors can thus be thought of as a loss of chaos, an event known to be preceded by distinct changes in the nonlinear properties of the HRR and pressure signals, such as their multifractality (Nair & Sujith 2014), permutation entropy (Domen *et al.* 2015), interdependence index (Chiocchini *et al.* 2017) and network structure (Murayama *et al.* 2018). Such changes have been used to develop early-warning indicators of thermoacoustic instability (Gotoda *et al.* 2014; Nair & Sujith 2014). However, despite its forecasting ability, chaos before the onset of thermoacoustic instability is not the focus of this study. Instead, we focus on how chaos arises after the onset of thermoacoustic instability, when the system is in a more dangerous state characterized by high-amplitude self-excited nonlinearly saturated oscillations.

1.2. *Routes to chaos*

The routes through which chaos arises in nonlinear dynamical systems have attracted broad scientific attention because understanding such routes can provide insight into how a system loses stability and transitions to complex states such as turbulence

(Gollub & Benson 1980). The following are three of the most common routes to chaos.

(i) *Period-doubling route*: Discovered by Feigenbaum (1978), this route to chaos involves a cascade of period-doubling bifurcations, resulting in the formation of a self-similar pattern in the bifurcation diagram (Hilborn 2000). In thermoacoustics, the period-doubling route to chaos has been observed both numerically (Subramanian *et al.* 2010; Kashinath *et al.* 2014; Huhn & Magri 2020) and experimentally (Sterling 1993).

(ii) *Ruelle–Takens–Newhouse (RTN) route*: Discovered by Newhouse, Ruelle & Takens (1978), this route to chaos involves the birth of a quasi-periodic attractor (3-torus) via three successive Hopf bifurcations. Such an attractor, with three incommensurate modes, is unstable to arbitrarily weak perturbations and will collapse into a chaotic attractor through a series of stretching and folding operations. In thermoacoustics, the RTN route to chaos has been observed both numerically (Kashinath *et al.* 2014; Huhn & Magri 2020) and experimentally (Boudy *et al.* 2012; Kabiraj *et al.* 2012, 2015; Vishnu *et al.* 2015).

(iii) *Intermittency route*: Discovered by Pomeau & Manneville (1980), this route to chaos involves intermittent alternation between regular and chaotic dynamics, despite all the system parameters remaining constant and free of significant external noise (Hilborn 2000). When a bifurcation parameter is just above its critical value, time traces show intermittent bursts of high-amplitude irregular motion amidst a background of low-amplitude regular motion. As the bifurcation parameter increases, the irregular bursts last longer in time until they eventually dominate the dynamics, leading to chaos.

In analyses of dissipative dynamical systems, Pomeau & Manneville (1980) identified three types of intermittency *en route* to chaos: type I (saddle-node bifurcation), type II (subcritical Hopf bifurcation) and type III (inverse period-doubling bifurcation). These were later joined by more types, such as on–off and crisis-induced intermittency (Hilborn 2000). In hydrodynamics (e.g. Rayleigh–Bénard convection), intermittency has a long history and has been named as a potential route to turbulence (Gollub & Benson 1980).

In thermoacoustics, however, the first evidence of intermittency was reported not too long ago by Kabiraj & Sujith (2012), who found type-II dynamics in a laminar premixed combustor after the onset of thermoacoustic instability – but not *en route* to chaos. In subsequent experiments on a turbulent premixed combustor, Nair *et al.* (2013, 2014) found intermittency before the onset of thermoacoustic instability: as the bifurcation parameter was varied, a quiescent background of low-amplitude aperiodic fluctuations gave way to increasingly long bursts of high-amplitude periodic oscillations associated with a limit cycle. Although those aperiodic fluctuations (combustion noise) showed signs of high-dimensional chaos (Tony *et al.* 2015), they arose before the onset of full-blown thermoacoustic instability, implying that the intermittency route to chaos has yet to be established in the self-excited regime of a thermoacoustic system.

1.3. *Contributions of the present study*

In nonlinear dynamics, the three classic routes to chaos are the period-doubling route, the RTN route and the intermittency route. Although the first two routes have previously been observed in self-excited thermoacoustic systems, the third

has not (§ 1.2). Here we present experimental evidence of the intermittency route to chaos in the self-excited regime of a prototypical thermoacoustic system – a laminar flame-driven Rijke tube. By establishing the last of the three classic routes to chaos, this study strengthens the universality of how strange attractors arise in self-excited thermoacoustic systems, paving the way for the application of generic suppression strategies based on chaos control (Schöll & Schuster 2008; Huhn & Magri 2020). Below, we describe our experimental set-up (§ 2) and present evidence of the intermittency route to chaos (§ 3), before concluding with the key implications of this study (§ 4).

2. Experimental set-up

Experiments are performed on a prototypical thermoacoustic system consisting of a laminar conical premixed flame in a tube combustor, i.e. a flame-driven Rijke tube. This system is identical to that used in our recent work on forced synchronization (Guan, Murugesan & Li 2018; Guan *et al.* 2019*a*,*b*), so only a brief overview is given here. The main features include a tube burner (inner diameter (ID) 16.8 mm; burner tip ID $D = 12$ mm; length 800 mm) mounted in a tube combustor (ID 44 mm; length $L = 860$ mm) with double open ends. The flame is produced with premixed reactants (air and liquefied petroleum gas) at an equivalence ratio of $\phi = 0.44$ ($\pm 3.2\%$), a bulk velocity of $\bar{u} = 1.4$ m s^{-1} ($\pm 0.2\%$), and a Reynolds number of $Re \equiv \rho \bar{u} D / \mu = 1130$ ($\pm 1.7\%$), where ρ and μ are the density and dynamic viscosity, respectively. The bifurcation parameter is the flame position, $\tilde{z} \equiv z/L$, where z is the distance between the burner tip and the combustor entrance. The system dynamics is determined from the acoustic pressure fluctuations in the combustor, $p'(t)$, which are measured with a probe microphone (GRAS 40SA, $\pm 2.5 \times 10^{-5}$ Pa) mounted at $\tilde{z} = 0.45$. For most tests, the microphone output is digitized at 16 384 Hz for 6 s on a 16-bit data converter. Further details on the experimental set-up can be found in Guan *et al.* (2018, 2019*a*,*b*).

3. Experimental results and discussion

3.1. *Intermittency route to chaos*

Figure 1 shows an overview of the system dynamics. On inspecting the bifurcation diagram (figure 1*a*) and the power spectral density (PSD; figure 1*b*), we find five different dynamical states as $\tilde{z}$ increases: a fixed point → a limit cycle → quasi-periodicity → intermittency → chaos. Below, we discuss these states briefly, before examining the intermittent state (§ 3.2) and the chaotic state (§ 3.3) in more detail.

(i) *Fixed point*: Initially ($0 \leqslant \tilde{z} < 0.034$, purple markers/lines), the system is not thermoacoustically unstable, i.e. it is not self-excited. This is because the coupling between the HRR oscillations of the flame and the acoustic pressure oscillations of the combustor is not strong enough to overcome the dissipation in the system (Lieuwen & Yang 2005). This assessment is supported by the absence of high-amplitude features in the bifurcation diagram (figure 1*a*) and the time trace (figure 1*c*1), and by the absence of dominant peaks in the PSD (figure 1*b*). It is also supported by the presence of a ball-like structure at the origin of the phase portrait (figure 1*c*2), which leads to a single cluster of trajectory intercepts in the two-sided Poincaré map (figure 1*c*3). If the system were free of noise, its time trace would be perfectly steady, and its phase trajectory would converge to a discrete point at the origin. These observations indicate that the system is residing on a fixed-point attractor perturbed by low levels of noise.
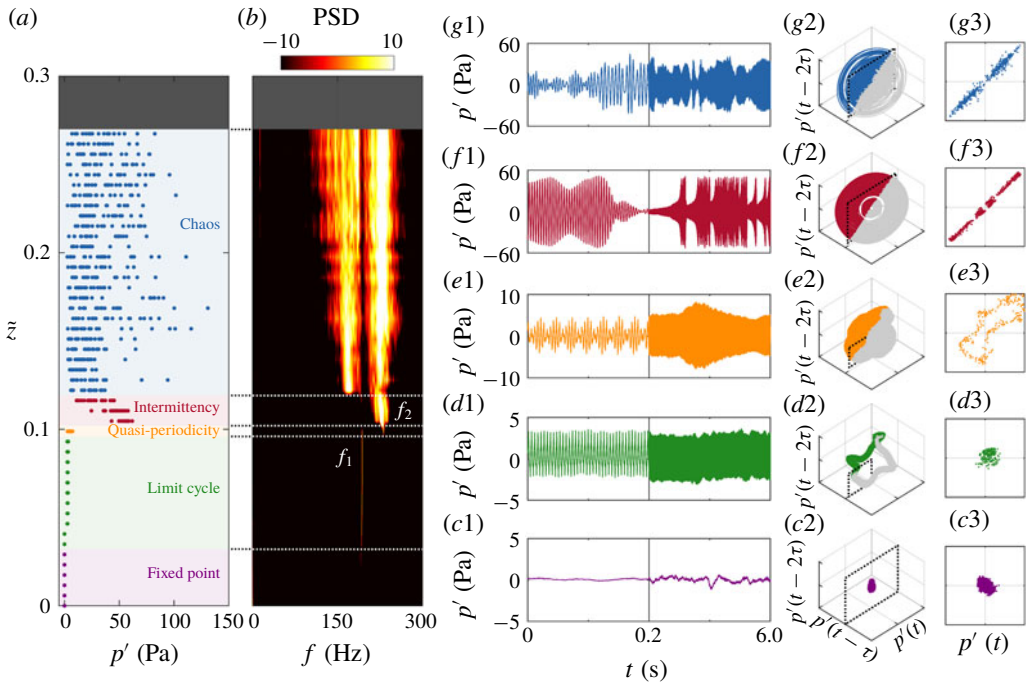
FIGURE 1. Overview of the system dynamics: (*a*) bifurcation diagram and (*b*) PSD of the combustor pressure fluctuations, $p'(t)$, as a function of the flame position, $\tilde{z}$. (*c*–*g*) Time traces (1), phase portraits (2) and Poincaré maps (3) for five dynamical states: (*c*) $\tilde{z} = 0$, a fixed point; (*d*) $\tilde{z} = 0.058$, a period-1 limit cycle; (*e*) $\tilde{z} = 0.099$, 2-torus quasi-periodicity; (*f*) $\tilde{z} = 0.116$, type-II intermittency; and (*g*) $\tilde{z} = 0.122$, low-dimensional chaos. The flame blows off at $\tilde{z} \geqslant 0.267$.

(ii) *Limit cycle*: At higher flame positions ($0.034 \leqslant \tilde{z} < 0.099$, green markers/lines), the system becomes thermoacoustically unstable (i.e. self-excited), having transitioned from a fixed point to a limit cycle via a Hopf bifurcation. This bifurcation is supercritical because the rise in the amplitude of $p'(t)$ above the Hopf point ($\tilde{z} = 0.034$), which marks the onset of thermoacoustic instability, is gradual rather than abrupt (figure 1*a*). The limit cycle produces a sharp peak at $f_1 \approx 191$ Hz in the PSD (figure 1*b*), near-sinusoidal oscillations in the time trace (figure 1*d*1), and a closed periodic orbit in the phase portrait (figure 1*d*2). The corresponding one-sided Poincaré map (figure 1*d*3) shows a single cluster of trajectory intercepts, indicating that the limit cycle is of period 1.

(iii) *Quasi-periodicity*: At slightly higher flame positions ($0.099 \leqslant \tilde{z} < 0.105$, orange markers/lines), the system remains thermoacoustically unstable, but admits a second self-excited natural mode. This can be seen in the PSD (figure 1*b*), where a new peak emerges at $f_2 \approx 231$ Hz alongside the peak at $f_1 \approx 191$ Hz from the original limit cycle. It can also be seen in the time trace (figure 1*e*1), which shows beating modulations characteristic of a self-excited oscillator with multiple modes (Li & Juniper 2013*a,b*). Because the two modes (f_1 and f_2) are not commensurate (i.e. their winding number is not rational), the trajectory in the phase portrait is not closed (figure 1*e*2), but spirals non-repeatedly on the surface of a stable ergodic two-dimensional quasi-periodic attractor (2-torus),

as evidenced by a closed ring in the one-sided Poincaré map (figure 1e3). These observations indicate that the system has transitioned from a period-1 limit cycle to an ergodic 2-torus quasi-periodic attractor via a Neimark–Sacker bifurcation.

(iv) *Intermittency*: At even higher flame positions ($0.105 \leqslant \tilde{z} < 0.122$, red markers/lines), the system exhibits intermittency. This is evidenced by the data points in the bifurcation diagram becoming more scattered as the system alternates between two different states (figure 1a): quasi-periodicity and chaos. This can be seen more clearly in the time trace (figure 1f1), where bursts of high-amplitude chaos appear intermittently over a background of medium-amplitude quasi-periodicity. Meanwhile, the second natural mode (f_2) strengthens relative to the first natural mode (f_1), dominating the PSD with a broad peak at f_2 (figure 1b). In phase space (figures 1f2 and 1f3), the system alternates between two different attractors: a 2-torus at the core and a strange attractor around it. If the phase trajectory is initially near the 2-torus (inner orbit), it remains there for some time and then bursts out to the strange attractor (outer orbit), before being re-injected to the 2-torus. This bursting and re-injection of the phase trajectory repeats intermittently, with the bursts of chaos lengthening in time as the bifurcation parameter ($\tilde{z}$) increases. The details of this intermittent state will be examined in § 3.2.

(v) *Chaos*: At the highest flame positions ($0.122 \leqslant \tilde{z} < 0.267$, blue markers/lines), the system becomes chaotic: the alternating epochs of quasi-periodicity and chaos observed during intermittency are replaced by a continuous regime of high-amplitude chaos (figure 1g1). This causes the data points in the bifurcation diagram to become even more scattered (figure 1a). In the PSD (figure 1b), the original natural mode (f_1) strengthens to match the second natural mode (f_2), with both modes being relatively broadband, a defining feature of chaos (Hilborn 2000). Both the phase portrait (figure 1g2) and the Poincaré map (figure 1g3) show complex non-repeating fractal structures, which suggests the presence of a strange attractor associated with chaos. In § 3.3, we will verify the strange chaotic nature of this state using additional tools from dynamical systems theory. It is worth mentioning that chaotic thermoacoustic oscillations can arise from two distinct physical mechanisms (Huhn & Magri 2020): (a) the nonlinear HRR response of a flame to incident acoustic perturbations, and (b) turbulence-induced modulation of the HRR dynamics via the hydrodynamic field. The first mechanism is likely to be dominant in our laminar combustor, as previous numerical simulations have shown that chaotic thermoacoustic oscillations can be produced by the nonlinear saturation of laminar flame models, without the action of turbulent hydrodynamics (Kashinath *et al.* 2014; Waugh, Kashinath & Juniper 2014; Orchini, Illingworth & Juniper 2015).

3.2. *Analysis of intermittency*

We analyse the intermittent state in more detail to better understand the route to chaos. We use a longer sampling time of 40 s to capture a sufficient number of alternation events for statistical convergence. Figures 2(a) and 2(b) show a 6 s window of the normalized pressure fluctuation signal ($\tilde{p}' \equiv p'/|p'|_{max}$) and its short-time PSD, respectively. Intermittent bursts of high-amplitude chaos can be seen amidst a background of medium-amplitude quasi-periodicity. The PSD of the chaotic bursts is characterized by a broad peak at f_2, whereas that of the quasi-periodic epochs is characterized by two relatively sharp peaks at f_1 and f_2, consistent with the phase trajectory evolving on an ergodic 2-torus.
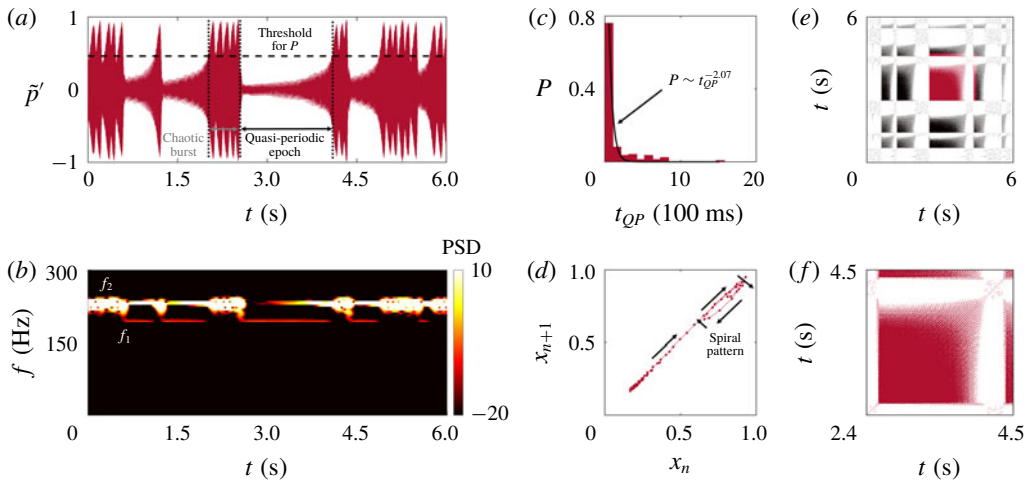
FIGURE 2. Evidence of type-II intermittency ($\tilde{z} = 0.116$): (*a*) a time trace of $p'(t)$ showing bursts of high-amplitude chaos amidst a background of medium-amplitude quasi-periodicity; (*b*) the short-time PSD, (*c*) the probability distribution of the quasi-periodic epoch durations, (*d*) the first return map, (*e*) the recurrence plot (RP), and (*f*) a magnified view of the RP showing a kite-like structure.

Next we quantify the intermittent dynamics using three proven techniques. First, we compute the probability distribution of the duration of the quasi-periodic epochs (t_{QP}) using the method of Hammer *et al.* (1994). This involves setting an amplitude threshold in the time trace ($\tilde{p}' = 0.5$; see the horizontal dashed line in figure 2*a*) and measuring the duration for which $\tilde{p}'$ is below this threshold. These t_{QP} values are then binned to create a histogram of the quasi-periodic durations P, as shown in figure 2(*c*). We find that P exhibits a power-law decay with an exponent of -2.07 (95 % confidence) at small t_{QP}, followed by an exponential tail at large t_{QP}. This behaviour indicates the presence of type-II intermittency, for which theory based on random re-injections predicts an initial power-law exponent of -2 (Schuster & Just 2006). By comparison, type-I intermittency is predicted to show a power-law decay with an exponent of $-1/2$ at small t_{QP} followed by an increase at large t_{QP}, while type-III intermittency is predicted to show a power-law decay with an exponent of $-3/2$ at small t_{QP} (Schuster & Just 2006).

Second, we examine the first return map (figure 2*d*), where a vector of successive local maxima within the quasi-periodic epochs (x_n) is plotted against a time-delayed version of itself (x_{n+1}). We find that the data points cluster on the main diagonal, moving from the bottom left to the top right, before forming a spiral pattern characteristic of type-II intermittency (Sacher, Elsässer & Göbel 1989). If this were type-I intermittency, the data points would cluster in a narrow channel off the main diagonal (Pomeau & Manneville 1980). If this were type-III intermittency, the data points would form a $\tan(x)$-like structure across the main diagonal (Schuster & Just 2006). The presence of a spiral pattern in the first return map is thus further evidence of type-II intermittency (Sacher *et al.* 1989).

Third, we examine the recurrence plot (RP). Introduced by Eckmann, Kamphorst & Ruelle (1987), RPs have been used throughout science and engineering to uncover hidden patterns in time-series data, including to distinguish between different types

of intermittency (Klimaszewska & Żebrowski [2009]). Figures 2(*e*) and 2(*f*) show the RP for our system and its magnified view (highlighted in red), respectively. These figures are generated using the algorithm of Klimaszewska & Żebrowski ([2009]), with an embedding dimension of $d = 10$, a time delay of $\tau = 2$ ms and a recurrence threshold of 10% of the largest attractor dimension. During bursts of high-amplitude chaos, the RP is sparsely populated (white regions), indicating little to no recurrence of the phase trajectory. As the system switches to an epoch of quasi-periodicity, a densely filled square with a stretched top-right corner emerges (figure 2*f*). In nonlinear dynamics, such a square is known as a kite-like structure and is a signature feature of type-II intermittency (Klimaszewska & Żebrowski [2009]). Similar kite-like structures have previously been observed in both laminar (Kabiraj & Sujith [2012]) and turbulent (Pawar *et al.* [2016]; Unni & Sujith [2017]) combustors with type-II intermittency.

In summary, by examining (i) the probability distribution of the quasi-periodic epoch durations, (ii) the first return map and (iii) the RP, we have shown that the intermittency observed *en route* to chaos is of type II from the Pomeau & Manneville ([1980]) scenario.

3.3. *Analysis of chaos*

As §3.1 has shown, analysis of the $p'(t)$ signal in the time, frequency and phase domains suggests the existence of chaos after intermittency. To verify the existence of chaos and to analyse its properties, we use four proven tools from dynamical systems theory. We apply these tools to both a chaotic state and a periodic state, the latter for comparison purposes.

First, we apply the permutation spectrum test proposed by Kulp & Zunino ([2014]), using an embedding dimension of $d = 4$ and a time delay of $\tau = 1.2$ ms, for 20 different subsets of the $p'(t)$ signal. For the periodic state (figures 3*a*1 and 3*b*1), the permutation spectra from the different subsets overlap reasonably well, with their standard deviation falling to zero ($\zeta \approx 0$) at many ordinal patterns, consistent with the limit-cycle nature of this state (Kulp & Zunino [2014]). For the chaotic state (figures 3*a*2 and 3*b*2), the permutation spectra are more scattered, resulting in $\zeta \approx 0$ at only three ordinal patterns: 3, 16 and 22 (see inset of figure 3*b*2). Crucially, these ordinal patterns form forbidden patterns with symbolic sequences of 1-3-2-4, 3-2-4-1 and 4-2-3-1, respectively. Such forbidden patterns are characteristic of deterministic chaos (Kulp & Zunino [2014]).

Second, we compute the correlation dimension ($\overline{D_c}$) using the algorithm of Grassberger & Procaccia ([1983]). This provides an estimate of the number of active degrees of freedom in the system, thus quantifying the topological self-similarity of the attractors. Figure 3(*c*) shows the local slope of the correlation sum ($D_c \equiv \partial \log C_N / \partial \log R$) as a function of the normalized hypersphere radius (R/R_{max}) for three embedding dimensions ($d = 10$, 12 and 14). For the periodic state (figure 3*c*1), D_c converges to an average of $\overline{D_c} \approx 1.0$ within the self-similar Euclidean scaling range ($10^{-1} \leqslant R/R_{max} \leqslant 10^{-0.4}$), indicating limit-cycle dynamics. For the chaotic state (figure 3*c*2), D_c converges to an average of $\overline{D_c} \approx 3.6$ within $10^{-1.8} \leqslant R/R_{max} \leqslant 10^{-1.2}$. Such a non-integer value of $\overline{D_c}$ indicates that the attractor is strange (Hilborn [2000]). Moreover, the relatively low value of $\overline{D_c}$ indicates that the chaotic dynamics is low-dimensional (Hilborn [2000]). Collectively, these findings are consistent with our earlier observations of broadband components in the PSD (figure 1*b*) and irregular geometrical structures in phase space (figure 1*g*3).
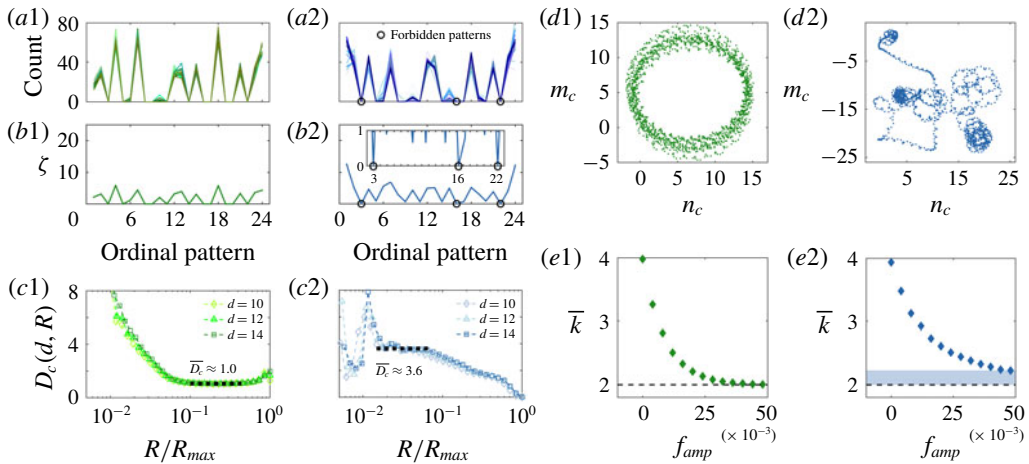
FIGURE 3. Evidence of low-dimensional chaos: (*a*) permutation spectra and (*b*) their standard deviation, (*c*) the local slope of the correlation sum as a function of the normalized hypersphere radius, (*d*) translation components from the 0–1 test, and (*e*) the mean degree of the filtered-horizontal visibility graph (f-HVG) as a function of the noise-filter amplitude. Data are shown for (green) a limit-cycle attractor at $\tilde{z} = 0.058$, and (blue) a strange attractor at $\tilde{z} = 0.122$.

Third, we use the 0–1 test from Gottwald & Melbourne (2004) to distinguish between non-chaotic and chaotic dynamics. This test has been successfully used to detect determinism in combustion noise (Nair *et al.* 2013) and self-excited thermoacoustic oscillations (Vishnu *et al.* 2015). We find that the translation components (m_c, n_c) undergo circular motion for the limit-cycle attractor (figure 3*d*1) but Brownian-like motion for the strange attractor (figure 3*d*2), indicating chaos in the latter. Although not shown here for brevity, the K value is close to zero for the limit-cycle attractor, but is around one for the strange attractor, further confirming the presence of chaos in the latter.

Fourth, we use the filtered-horizontal visibility graph (f-HVG) from Nuñez *et al.* (2012) to distinguish between periodic and chaotic dynamics. Visibility graphs were introduced in thermoacoustics by Murugesan & Sujith (2015). The f-HVG works by converting a time series into network structures via graph theory. For the limit-cycle attractor (figure 3*e*1), we find that the mean degree $\bar{k}$ converges to exactly 2 as the noise-filter amplitude f_{amp} increases, indicating a temporal period of $T = 1$, which is consistent with our earlier assessment (§ 3.1) that this limit cycle is of period 1. For the strange attractor (figure 3*e*2), we find that $\bar{k}$ has not yet converged to 2, despite the noise-filter amplitude being at a value ($f_{amp} = 0.05$) high enough to induce $\bar{k} = 2$ in the limit-cycle attractor. This absence of convergence in $\bar{k}$ is consistent with chaos (Nuñez *et al.* 2012).

In summary, by considering (i) the permutation spectrum test, (ii) the correlation dimension, (iii) the 0–1 test and (iv) the f-HVG, we have established the existence of a self-excited state of low-dimensional chaos on a strange attractor. When combined with the evidence from § 3.2, this confirms a transition to chaos via type-II intermittency.

4. Conclusions

In this experimental study, we have presented evidence of the intermittency route to chaos in the self-excited regime of a prototypical laminar thermoacoustic system. On increasing the bifurcation parameter $\tilde{z}$, we find five different dynamical states: a fixed point $\rightarrow$ a period-1 limit cycle $\rightarrow$ 2-torus quasi-periodicity $\rightarrow$ type-II intermittency from the Pomeau & Manneville (1980) scenario $\rightarrow$ low-dimensional chaos. The intermittent state is characterized by bursts of high-amplitude chaos appearing intermittently over a background of medium-amplitude quasi-periodicity. The type-II nature of this state is confirmed by: (i) a power-law decay in the probability distribution of the quasi-periodic epoch durations, with an exponent close to the theoretically predicted value of -2 at small t_{QP}; (ii) a spiralling trajectory in the first return map; and (iii) kite-like structures in the RP. The presence of low-dimensional chaos is confirmed by: (i) forbidden patterns in the permutation spectrum test; (ii) a non-integer correlation dimension of $\overline{D_c} \approx 3.6$; (iii) Brownian-like motion in the translation components of the 0–1 test, along with $K \approx 1$; and (iv) a non-convergent mean degree in the f-HVG. Together, these indicators provide compelling evidence of a transition to low-dimensional chaos via type-II intermittency.

Establishing the intermittency route to chaos is important because it is the last of the three classic routes to chaos to be discovered in self-excited thermoacoustic systems, the other two being the period-doubling route and the RTN route. This study thus strengthens the universality of how strange attractors arise in self-excited thermoacoustic systems, setting the stage for the application of generic suppression methods based on chaos control (Schöll & Schuster 2008; Huhn & Magri 2020).

As a final remark, it is worth recalling that, although intermittency involving chaos has previously been observed in the low-amplitude (combustion noise) regime of thermoacoustic systems (Nair *et al.* 2013, 2014), it has not, until now, been observed in the high-amplitude (self-excited) regime. This is an important distinction because, in practical combustors, the high-amplitude pressure oscillations arising after the onset of thermoacoustic instability have a greater potential to inflict mechanical damage and impair flame stability than the low-amplitude fluctuations associated with combustion noise (Lieuwen & Yang 2005). Crucially, if those high-amplitude oscillations happen to be chaotic, with their kinetic energy distributed over a broad range of frequencies, then they will have a greater potential to couple with the natural structural modes of the combustor hardware, producing more destructive fatigue loads via resonance (Suresh 1998). Here we have shown that chaos can arise via intermittency in the self-excited regime, after the onset of thermoacoustic instability. This implies that many of the early-warning indicators used to forecast the onset of limit-cycle oscillations based on a loss of chaos in the combustion-noise regime (Gotoda *et al.* 2014; Nair & Sujith 2014; Juniper & Sujith 2018) may be repurposed to forecast the onset of chaotic oscillations in the self-excited regime. The extent to which this can be achieved, particularly in turbulent combustors, remains to be determined.

Acknowledgements

Declaration of interests

The authors report no conflict of interest.

References

BOUDY, F., DUROX, D., SCHULLER, T. & CANDEL, S. 2012 Nonlinear flame describing function analysis of galloping limit cycles featuring chaotic states in premixed combustors. In *ASME Turbo Expo*, pp. 713–724. American Society of Mechanical Engineers.

CHIOCCHINI, S., PAGLIAROLI, T., CAMUSSI, R. & GIACOMAZZI, E. 2017 Chaotic and linear statistics analysis in thermoacoustic instability detection. *J. Propul. Power* **34** (1), 15–26.

DOMEN, S., GOTODA, H., KURIYAMA, T., OKUNO, Y. & TACHIBANA, S. 2015 Detection and prevention of blowout in a lean premixed gas-turbine model combustor using the concept of dynamical system theory. *Proc. Combust. Inst.* **35** (3), 3245–3253.

ECKMANN, J. P., KAMPHORST, S. O. & RUELLE, D. 1987 Recurrence plots of dynamical systems. *Eur. Phys. Lett.* **4** (9), 973–977.

FEIGENBAUM, M. J. 1978 Quantitative universality for a class of nonlinear transformations. *J. Stat. Phys.* **19** (1), 25–52.

FICHERA, A., LOSENNO, C. & PAGANO, A. 2001 Experimental analysis of thermo-acoustic combustion instability. *Appl. Energ.* **70** (2), 179–191.

GOLLUB, J. P. & BENSON, S. V. 1980 Many routes to turbulent convection. *J. Fluid Mech.* **100** (3), 449–470.

GOTODA, H., NIKIMOTO, H., MIYANO, T. & TACHIBANA, S. 2011 Dynamic properties of combustion instability in a lean premixed gas-turbine combustor. *Chaos* **21** (1), 013124.

GOTODA, H., SHINODA, Y., KOBAYASHI, M., OKUNO, Y. & TACHIBANA, S. 2014 Detection and control of combustion instability based on the concept of dynamical system theory. *Phys. Rev.* E **89** (2), 022910.

GOTTWALD, G. A. & MELBOURNE, I. 2004 A new test for chaos in deterministic systems. *Proc. R. Soc. Lond.* A **460** (2042), 603–611.

GRASSBERGER, P. & PROCACCIA, I. 1983 Characterization of strange attractors. *Phys. Rev. Lett.* **50** (5), 346–349.

GUAN, Y., GUPTA, V., KASHINATH, K. & LI, L. K. B. 2019a Open-loop control of periodic thermoacoustic oscillations: experiments and low-order modelling in a synchronization framework. *Proc. Combust. Inst.* **37**, 5315–5323.

GUAN, Y., GUPTA, V., WAN, M. & LI, L. K. B. 2019b Forced synchronization of quasiperiodic oscillations in a thermoacoustic system. *J. Fluid Mech.* **879**, 390–421.

GUAN, Y., LI, L. K. B., AHN, B. & KIM, K. T. 2019c Chaos, synchronization, and desynchronization in a liquid-fueled diffusion-flame combustor with an intrinsic hydrodynamic mode. *Chaos* **29** (5), 053124.

GUAN, Y., MURUGESAN, M. & LI, L. K. B. 2018 Strange nonchaotic and chaotic attractors in a self-excited thermoacoustic oscillator subjected to external periodic forcing. *Chaos* **28** (9), 093109.

HAMMER, P. W., PLATT, N., HAMMEL, S. M., HEAGY, J. F. & LEE, B. D. 1994 Experimental observation of on-off intermittency. *Phys. Rev. Lett.* **73** (8), 1095.

HILBORN, R. C. 2000 *Chaos and Nonlinear Dynamics*. Oxford University Press.

HUHN, F. & MAGRI, L. 2020 Stability, sensitivity and optimisation of chaotic acoustic oscillations. *J. Fluid Mech.* **882**, A24.

JUNIPER, M. P. & SUJITH, R. I. 2018 Sensitivity and nonlinearity of thermoacoustic oscillations. *Annu. Rev. Fluid Mech.* **50**, 661–689.

KABIRAJ, L., SAURABH, A., KARIMI, N., SAILOR, A., MASTORAKOS, E., DOWLING, A. P. & PASCHEREIT, C. O. 2015 Chaos in an imperfectly premixed model combustor. *Chaos* **25** (2), 023101.

KABIRAJ, L., SAURABH, A., WAHI, P. & SUJITH, R. I. 2012 Route to chaos for combustion instability in ducted laminar premixed flames. *Chaos* **22** (2), 023129.

KABIRAJ, L. & SUJITH, R. I. 2012 Nonlinear self-excited thermoacoustic oscillations: intermittency and flame blowout. *J. Fluid Mech.* **713**, 376–397.

KASHINATH, K., WAUGH, I. C. & JUNIPER, M. P. 2014 Nonlinear self-excited thermoacoustic oscillations of a ducted premixed flame: bifurcations and routes to chaos. *J. Fluid Mech.* **761**, 399–430.

KEANINI, R., YU, K. & DAILY, J. 1989 Evidence of a strange attractor in ramjet combustion. In *27th AIAA Aerospace Sciences Meeting*, p. 624. American Institute of Aeronautics and Astronautics.

KLIMASZEWSKA, K. & ŻEBROWSKI, J. J. 2009 Detection of the type of intermittency using characteristic patterns in recurrence plots. *Phys. Rev.* E **80** (2), 026214.

KULP, C. W. & ZUNINO, L. 2014 Discriminating chaotic and stochastic dynamics through the permutation spectrum test. *Chaos* **24** (3), 033116.

LEI, S. & TURAN, A. 2009 Nonlinear/chaotic behaviour in thermo-acoustic instability. *Combust. Theor. Model.* **13** (3), 541–557.

LI, L. K. B. & JUNIPER, M. P. 2013a Lock-in and quasiperiodicity in a forced hydrodynamically self-excited jet. *J. Fluid Mech.* **726**, 624–655.

LI, L. K. B. & JUNIPER, M. P. 2013b Phase trapping and slipping in a forced hydrodynamically self-excited jet. *J. Fluid Mech.* **735**, R5.

LIEUWEN, T. C. & YANG, V. 2005 *Combustion Instabilities in Gas Turbine Engines*. American Institute of Aeronautics and Astronautics.

MURAYAMA, S., KINUGAWA, H., TOKUDA, I. T. & GOTODA, H. 2018 Characterization and detection of thermoacoustic combustion oscillations based on statistical complexity and complex-network theory. *Phys. Rev.* E **97** (2), 022223.

MURUGESAN, M. & SUJITH, R. I. 2015 Combustion noise is scale-free: transition from scale-free to order at the onset of thermoacoustic instability. *J. Fluid Mech.* **772**, 225–245.

NAIR, V. & SUJITH, R. I. 2014 Multifractality in combustion noise: predicting an impending combustion instability. *J. Fluid Mech.* **747**, 635–655.

NAIR, V., THAMPI, G., KARUPPUSAMY, S., GOPALAN, S. & SUJITH, R. I. 2013 Loss of chaos in combustion noise as a precursor of impending combustion instability. *Intl J. Spray Combust.* **5** (4), 273–290.

NAIR, V., THAMPI, G. & SUJITH, R. I. 2014 Intermittency route to thermoacoustic instability in turbulent combustors. *J. Fluid Mech.* **756**, 470–487.

NEWHOUSE, S., RUELLE, D. & TAKENS, F. 1978 Occurrence of strange Axiom A attractors near quasiperiodic flows on t^m, $m \geqslant 3$. *Commun. Math. Phys.* **64** (1), 35–40.

NUÑEZ, A., LACASA, L., VALERO, E., GÓMEZ, J. P. & LUQUE, B. 2012 Detecting series periodicity with horizontal visibility graphs. *Intl J. Bifurcation Chaos* **22** (07), 1250160.

ORCHINI, A., ILLINGWORTH, S. J. & JUNIPER, M. P. 2015 Frequency domain and time domain analysis of thermoacoustic oscillations with wave-based acoustics. *J. Fluid Mech.* **775**, 387–414.

PAWAR, S. A., VISHNU, R., VADIVUKKARASAN, M., PANCHAGNULA, M. V. & SUJITH, R. I. 2016 Intermittency route to combustion instability in a laboratory spray combustor. *Trans. ASME J. Engng Gas Turbines Power* **138** (4), 041505.

POINSOT, T. 2017 Prediction and control of combustion instabilities in real engines. *Proc. Combust. Inst.* **36** (1), 1–28.

POMEAU, Y. & MANNEVILLE, P. 1980 Intermittent transition to turbulence in dissipative dynamical systems. *Commun. Math. Phys.* **74** (2), 189–197.

SACHER, J., ELSÄSSER, W. & GÖBEL, E. O. 1989 Intermittency in the coherence collapse of a semiconductor laser with external feedback. *Phys. Rev. Lett.* **63** (20), 2224–2227.

SCHÖLL, E. & SCHUSTER, H. G. 2008 *Handbook of Chaos Control*. John Wiley & Sons.

SCHUSTER, H. G. & JUST, W. 2006 *Deterministic Chaos*. John Wiley & Sons.

STERLING, J. D. 1993 Nonlinear analysis and modelling of combustion instabilities in a laboratory combustor. *Combust. Sci. Technol.* **89** (1–4), 167–179.

SUBRAMANIAN, P., MARIAPPAN, S., SUJITH, R. I. & WAHI, P. 2010 Bifurcation analysis of thermoacoustic instability in a horizontal Rijke tube. *Intl J. Spray Combust.* **2**, 325–355.

SURESH, S. 1998 *Fatigue of Materials*. Cambridge University Press.

TONY, J., GOPALAKRISHNAN, E. A., SREELEKHA, E. & SUJITH, R. I. 2015 Detecting deterministic nature of pressure measurements from a turbulent combustor. *Phys. Rev.* E **92** (6), 062902.

UNNI, V. R. & SUJITH, R. I. 2017 Flame dynamics during intermittency in a turbulent combustor. *Proc. Combust. Inst.* **36** (3), 3791–3798.

VISHNU, R., SUJITH, R. I. & AGHALAYAM, P. 2015 Role of flame dynamics on the bifurcation characteristics of a ducted V-flame. *Combust. Sci. Technol.* **187** (6), 894–905.

WAUGH, I. C., KASHINATH, K. & JUNIPER, M. P. 2014 Matrix-free continuation of limit cycles and their bifurcations for a ducted premixed flame. *J. Fluid Mech.* **759**, 1–27.